

SCIENTIFIC REPORTS



OPEN

Psiguajadials A–K: Unusual *Psidium* Meroterpenoids as Phosphodiesterase-4 Inhibitors from the Leaves of *Psidium guajava*

Gui-Hua Tang, Zhen Dong, Yan-Qiong Guo, Zhong-Bin Cheng, Chu-Jun Zhou & Sheng Yin

Bioassay-guided fractionation of the ethanolic extract of the leaves of *Psidium guajava* led to the isolation of 11 new *Psidium* meroterpenoids, psiguajadials A–K (1–11), along with 17 known ones (12–28). Their structures and absolute configurations were elucidated by spectroscopic methods and comparison of experimental and calculated ECD. Compounds 1 and 2 represent two unprecedented skeletons of 3,5-diformyl-benzyl phloroglucinol-coupled sesquiterpenoid, while 3 is the first example of *Psidium* meroterpenoids coupling via an oxepane ring. Putative biosynthetic pathways towards 1 and 2 are proposed. Compounds 1–13 and 16–26 exhibited moderate inhibitory activities against phosphodiesterase-4 (PDE4), a drug target for asthma and chronic obstructive pulmonary disease, with IC_{50} values in the range of 1.34–7.26 μ M.

Phloroglucinol-coupled mono- or sesquiterpenoids are a group of structurally diverse meroterpenoids mainly occurring in species of the genera *Eucalyptus*, *Psidium*, *Rhodomyrtus*, *Myrtus* (Myrtaceae), and *Hypericum* (Guttiferae)^{1–17}. Biosynthetically, they are proposed to be adducts of phloroglucinol derivatives and terpenoids via hetero-Diels-Alder or carbocation-induced stepwise reactions^{6,10}. So far more than 100 phloroglucinol-coupled terpenoids have been reported^{11,18}, and their intriguing structures and important biological activities have attracted broad interest from both natural products and synthetic chemists over the last half century^{5,19–24}. For instance, psiguajadials A, C, and D^{9,10}, hyperjaponones A–E¹⁶, and hyperjaponols A and C¹⁷ with novel skeletons and appealing pharmacological activities (e.g., antitumor and antiviral properties) have been synthesized by several groups^{25,26}. *Psidium* meroterpenoids are a subgroup of this compound class, which are exclusively reported from the species *Psidium guajava*. Structurally, they are characterized by the presences of 3,5-diformyl-benzyl phloroglucinol moiety and a dihydropyran ring junction. Recently, a number of excellent articles on the separation or biomimetic total synthesis of *Psidium* meroterpenoids have increased the interest in the study of this type of compounds^{8,25,27}.

Phosphodiesterase-4 (PDE4), which specifically catalyzes the hydrolysis of the second messenger cyclic adenosine monophosphate (cAMP), is a therapeutic target of high interest for central nervous system (CNS), inflammatory, and respiratory diseases²⁸. Although a number of structurally diverse PDE4 inhibitors have been developed over the last decade, roflumilast is the only one that successfully launched on the market to treat asthma and chronic obstructive pulmonary disease²⁹. However, the wide clinical use of roflumilast has been limited by the dose-limiting side effects, such as diarrhea, nausea, headaches, and weight loss. Therefore, the discovery of novel PDE4 inhibitors with stronger potency and less side-effects continues unabated.

In our continuing search for novel PDE4 inhibitors from Chinese herbs^{30–32}, a fraction of the 95% aqueous ethanol extract of *Psidium guajava* exhibited moderate inhibitory effect on PDE4 (inhibitory rate >50% at 10 μ g/mL). Subsequent chemical investigation of this fraction led to the isolation of 28 *Psidium* meroterpenoids including 11 new ones (1–11). Bioassay verified that most of these meroterpenoids were responsible for the activity of the crude fraction. Herein, we report the isolation, structure elucidation, putative biosynthetic origin, and PDE4 inhibitory activities of these metabolites.

School of Pharmaceutical Sciences, Sun Yat-sen University, Guangzhou, 510006, People's Republic of China. G.H. Tang and Z. Dong contributed equally to this work. Correspondence and requests for materials should be addressed to S.Y. (email: yinsh2@mail.sysu.edu.cn)

Results and Discussion

Leaves of *P. guajava* (6.0 kg) was extracted with 95% EtOH at room temperature (rt) to give a residue, which was suspended in H₂O and partitioned with EtOAc and *n*-BuOH, respectively. Subsequent purification of the EtOAc fraction with various column chromatographic methods afforded compounds **1**–**28** (Fig. 1).

Psiguajadial A (**1**), a colourless oil, had a molecular formula of C₃₀H₃₄O₅ as determined by the HR-ESI-MS ion at *m/z* 473.2304 [M – H][–] (calcd 473.2333), corresponding to 14 degrees of unsaturation (DOUs). The IR absorption bands revealed the presence of OH (3448 cm^{–1}) and conjugated carbonyl (1633 cm^{–1}) groups. The ¹H NMR data (Table 1) displayed signals for three secondary methyl groups [δ_{H} 1.00 (3H, d, *J* = 6.3 Hz), 0.89 (3H, d, *J* = 6.6 Hz), and 0.85 (3H, d, *J* = 6.6 Hz)], two formyl groups [δ_{H} 10.13 and 10.12 (each 1H, s)], two chelated phenolic hydroxyls [δ_{H} 13.55 and 13.19 (each 1H, s)], a monosubstituted benzene ring [δ_{H} 7.14–7.28 (5H, m)], and a series of aliphatic multiplets. The ¹³C NMR spectrum, associated with DEPT experiments, resolved 30 carbon resonances attributable to two conjugated aldehydes (δ_{C} 192.2 and 191.6), a monosubstituted phenyl [δ_{C} 144.6, 128.6 ($\times 2$), 126.7 ($\times 2$), and 126.3], a hexasubstituted phenyl, three sp³ methyls, five sp³ methylenes, six sp³ methines, and two sp³ quaternary carbons (one oxygenated). The collective information suggested that **1** was a *Psidium* meroterpenoid possessing the basic structural features of a cubebane sesquiterpenoid unit³³ and a 3,5-diformyl-benzyl phloroglucinol substructure⁶.

Detailed 2D NMR analysis (¹H–¹H COSY, HSQC, HMBC, and NOESY) further confirmed the presence of these moieties. In particular, two structural fragments **a** (C-2–C-3) and **b** (from C-5 to C-14) were first established by the ¹H–¹H COSY correlations (Fig. 2). The connectivities of **a**, **b**, the methylene (C-15), and two sp³ quaternary carbons (C-4 and C-5) were achieved by the HMBC correlations of H₃-14/C-1, H-10/C-2, H-5/C-2, C-3, C-4, C-10, and C-15, and H₂-15/C-3, C-4, and C-5 (Fig. 2), which led to the identification of the cubebane moiety. The HMBC correlations from two phenolic hydroxyls (5'-OH and 7'-OH) and two formyl protons (H-14' and H-15') to C-5', C-7', C-4', and C-6' of a benzene ring, respectively, together with the NOE correlations of H-15'/5'-OH and 7'-OH, and H-14'/5'-OH outlined a 3,5-diformyl phloroglucinol fragment. The aforementioned fragment and a mono-substituted benzene ring were connected to C-1' by the HMBC correlations of H-1'/C-2', C-3', C-7', C-8', C-9', and C-13' to generate a 3,5-diformyl-benzyl phloroglucinol moiety. The connection between cubebane and 3,5-diformylbenzyl phloroglucinol moieties *via* C-1'–C-15 bond was identified by ¹H–¹H COSY correlations of H-1'/H-15. As 13 of the 14 DOUs were accounted for by two aldehydes, two benzene rings, and three rings of cubebane, the remaining DOU required the presence of an additional ring in **1**. Although no direct HMBC correlations were available to construct the additional ring, the still “loose ends” of an oxygenated quaternary carbon (δ_{C} 89.8, C-4) and a downfield-shifted aromatic carbon (δ_{C} 165.8, C-3') suggested that an oxygen bridge was located between C-4 and C-3' to form a dihydropyran ring. This was further supported by the NOE correlation between H-13 (12) and H-14'. Thus, a planar structure of **1** was proposed as depicted in Fig. 2, which was fully consistent with its molecular composition. Compound **1** represents a new skeleton of sesquiterpenoid-based *Psidium* meroterpenoid with the presence of cubebane moiety in this compound class for the first time.

The relative configuration of **1** was established on the basis of NOESY experiments (recorded in both CDCl₃ and pyridine-*d*₅) and ¹H–¹H coupling constant analysis. The NOE correlations of H-5/H-7, H-9 α , and H₃-14 indicated that these protons or functional groups were cofacial and were arbitrarily assigned α -orientations (Fig. 3). Accordingly, the NOE correlations of H-6/H-3 β and H-11 designated H-6 to be β -oriented. The *trans*-relationship of H-5 and H-6 on the cyclopropane ring was further supported by the small coupling constant (*J* = 2.9 Hz) between them³³. Finally, the β -orientation of C-4–O–C-3' bond at the spirocenter and the α -orientation of H-1' were assigned by NOE correlations of H-5/H-1' and H₃-13(12)/H-14', respectively.

To determine the absolute configuration of **1**, the experimental ECD spectrum of **1** was compared with those calculated for its isomers by the TDDFT method. In Fig. 4, the experimental ECD spectrum of **1** showed sequential positive, positive, negative, and negative Cotton effects at 340, 283, 250, and 212 nm, respectively, which matched the calculated ECD curve for **1a**, the isomer with the 1*R*, 4*R*, 5*R*, 6*R*, 7*S*, 10*R*, 1'*R* absolute configuration, indicating that **1** possessed the same absolute configuration as **1a**.

Psiguajadial B (**2**), a colourless oil, exhibited a molecular formula of C₃₀H₃₄O₅ as determined by HR-ESI-MS at *m/z* 475.2475 [M + H]⁺ (calcd 475.2479), indicating that it was an isomer of **1**. The 1D NMR spectra of **2** (Tables 1 and 2) exhibited most of the structural features found in **1**, especially those for a cubebane moiety and a 3,5-diformylbenzyl phloroglucinol unit, indicating that **2** is comprised of the same coupling units as **1**, with differences being due to the coupling patterns. Detailed 2D NMR analysis (¹H–¹H COSY, HMBC, and NOESY) (Fig. 2) further confirmed this fact. The benzyl methine (CH-1') of the 3,5-diformylbenzyl phloroglucinol moiety was first established by HMBC correlations of H-1'/C-9' (13'), C-3', and C-7' and H-9'(13')/C-1'. Then a methine from the cubebane moiety which showed the ¹H–¹H COSY correlation with a methylene (CH₂-2) and the HMBC correlation with a tertiary methyl (CH₃-15) was assigned as CH-3. The cubebane and phloroglucinol moieties were connected by ¹H–¹H COSY correlation of H-1'/H-3, revealing a C-3–C-1' coupling pattern in **2**. The presence of the oxygen bridge between C-4 and C-3' was determined using the same way as described for **1**. Therefore, the planar structure of **2** was established as shown in Fig. 2, which represents another new skeleton of cubebane-based *Psidium* meroterpenoid with a C-1'–C-3 linkage rather than the C-1'–C-15 linkage in **1**.

The relative configuration of **2** was established by NOESY analysis. The key NOE correlations (Fig. 3) of H-5/H-7, H-9 α , and H₃-14 suggested that H-5, H-7, H-9 α , and the H₃-14 were cofacial and were arbitrarily assigned the α -orientation. Thus, the β -orientation of H-3, H-6, CH₃-15, and the phenyl group were established by the NOE correlations of H-6/H-11, H-3, and H-2 β , and H₃-15/H-3 and H-9' (13'). The small coupling constant (*br. s*) between H-5 and H-6 further confirmed the *trans*-relationship of these protons on the cyclopropane ring³³. The absolute configuration of **2** was deduced to be 1*R*, 3*S*, 4*R*, 5*R*, 6*R*, 7*S*, 10*R*, 1'*R* by comparison of its experimental ECD spectrum with those of the calculated for the isomers (Fig. 5).

Psiguajadial C (**3**) was assigned the molecular formula C₃₀H₃₂O₅ based on the HR-ESI-MS and NMR data. The 1D NMR spectra of **3** (Tables 1 and 2) exhibited most of the structural features found in psiguajadial A (**16**)⁹, a

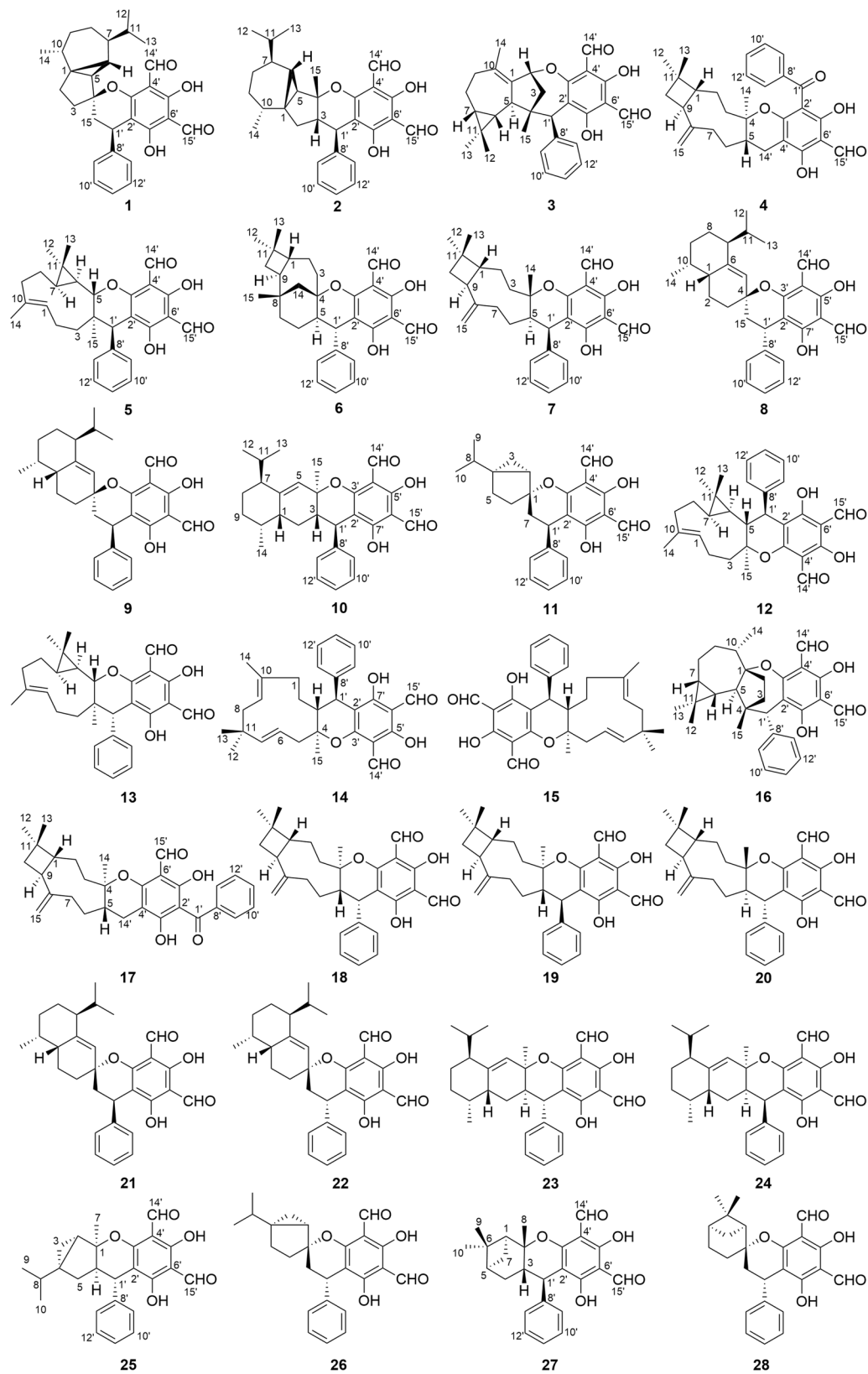


Figure 1. Structures of compounds 1–28.

known globulane-based *Psidium* meroterpenoid featuring a rare oxocane ring junction, except that a methylene (δ_C 36.6, C-2), an oxygenated quaternary carbon (δ_C 104.1, C-1) and an upfielded methine (δ_C 39.9, C-10) in 16

Position	1	2	3	4
1	—	—	—	1.66, m
2	α 1.82, m; β 1.59, m	β 1.96, dd (12.8, 7.9); α 1.77, t (12.0)	5.50, d (4.7)	0.92, m
3	β 1.77, m; α 1.60, m	2.28, t (9.3)	a 2.45, d (14.5); b 1.54, dd (14.5, 4.0)	β 1.60, m; α 0.90, m
5	1.13, d (2.9)	1.19, br. s	2.27, m	1.82, m
6	1.04, m	0.64, br. s	0.77, t (10.3)	β 1.57, m; α 1.49, m
7	0.84, m	1.00, m	0.57, m	α 2.36, m; β 2.03, m
8	α 1.40, m; β 0.81, m	α 1.42, m; β 0.83, m	β 1.67, m; α 1.54, m	—
9	β 1.65, m; α 0.53, dddd (12.1, 12.1, 12.1, 1.9)	β 1.61, m; α 0.51, q (12.4)	α 2.26, m; β 2.16, m	2.27, m
10	1.71, m	1.70, m	—	α 1.61, m; β 1.56, m
11	1.52, m	1.56, m	—	—
12	0.89, d (6.6)	0.93, d (6.6)	β 1.02, s	α 0.87, s
13	0.85, d (6.6)	0.90, d (6.7)	α 1.15, s	β 0.93, s
14	1.00, d (6.3)	0.75, d (6.2)	1.72, s	1.00, s
15	α 2.27, dd (14.1, 7.2); β 1.99, dd (14.1, 10.4)	1.08, s	1.08, s	4.83, br.s; 4.80, br.s
1'	4.17, dd (10.4, 7.2)	4.20, br. s	4.39, br. s	—
9'/13'	7.14, m	7.09, d (7.5)	7.27, m	7.40, m
10'/12'	7.28, m	7.28, t (7.5)	7.24, m	7.39, m
11'	7.21, m	7.20, t (7.5)	7.19, t (6.7)	7.47, m
14'	10.12, s	10.18, s	10.22, s	α 2.61, dd (16.6, 5.4); β 2.00, dd (16.6, 12.1)
15'	10.13, s	10.16, s	10.10, s	10.23, s
5'-OH	13.55, s	13.61, s	13.53, s	13.23, s
7'-OH	13.19, s	13.23, s	13.44, s	13.71, s

Table 1. ^1H NMR (400 Hz) data of compounds **1–4** in CDCl_3 (δ in ppm, J in Hz).

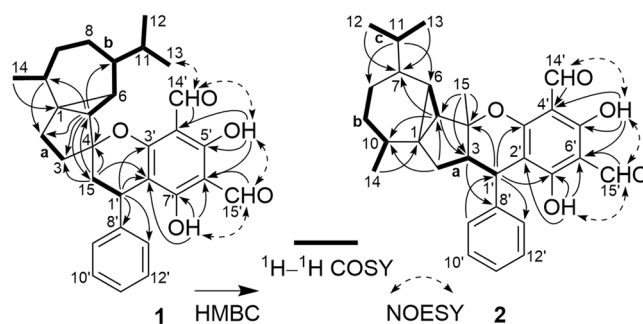


Figure 2. Selected ^1H - ^1H COSY, HMBC, and NOESY correlations of **1** and **2**.

were replaced by a oxygenated methine (δ_{C} 85.5, C-2) and a tetra-substituted double bond (δ_{C} 138.2 and 136.0, C-1 and C-10) in **3**. This indicated that the oxygen bridge started from C-1 in **16** was migrated to C-2 with the formation of $\Delta^{1(10)}$ in **3**, which was further confirmed by the HMBC correlations (Fig. 6) from H_3 -14 to C-1, C-9, and C-10 and from H-2 to C-3', C-1, and C-10. The relative configuration of **3** was assigned by the NOE analysis (Fig. 7). The NOE correlations of H-3b/H-2, H-6, and H_3 -15, H-3a/H-2, H_3 -15, and H-13' (9'), H_3 -12/H-6 and H-7, and H_3 -15/H-9' (13') indicated that H-2, H-6, H-7, CH_3 -12, CH_3 -15, the phenyl group, and the C-2–C-3–C-4 bridge were cofacial and were arbitrarily assigned β -orientations. Thus, the α -orientation of H-5, H_3 -13, and H-1' was deduced by the NOE correlations of H-5/ H_3 -13 and H-1'. The absolute configuration of **3** was established as 2*R*, 4*S*, 5*R*, 6*R*, 7*R*, 1'*R* by comparison of its experimental ECD spectrum with those of the calculated isomers (Fig. 8). Compound **3** represents the first example of *Psidium* meroterpenoid coupling via an oxepane ring.

Psiguajadial D (**4**) possessed the molecular formula $\text{C}_{30}\text{H}_{34}\text{O}_5$ as determined by its HR-ESI-MS and 1D NMR data. The ^1H and ^{13}C NMR data of **4** bore a high resemblance to those of guapsidial A (**17**)¹¹, with the major differences occurring at C-3', C-7', and C-8' of the benzoyl-phloroglucinol moiety ($\Delta\delta_{\text{C}} = 2.3, 1.9, \text{ and } 1.6$ ppm, respectively), indicating that **4** possessed a different substitution pattern at the phloroglucinol unit. The locations of 5'-OH, 7'-OH, and 15'-CHO were assigned by HMBC correlations from the corresponding protons to C-5', C-7', and C-6', respectively (Fig. 6). Consequently, the benzoyl group was located at the only remaining position on the phloroglucinol ring (C-2'). This was further supported by the NOE cross-peaks of H-15'/5'-OH and 7'-OH

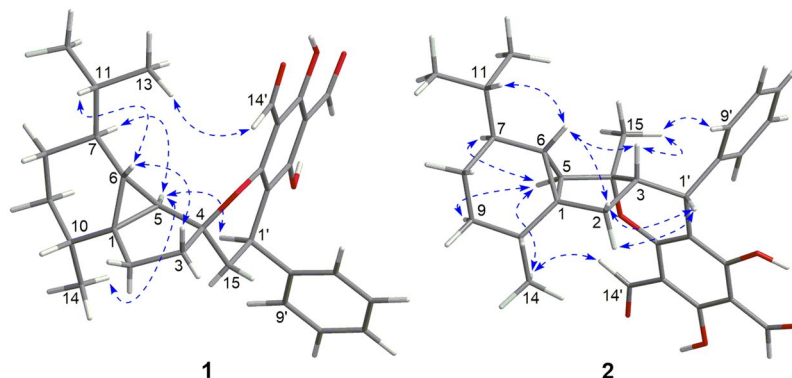


Figure 3. Selected NOESY correlations of **1** and **2**.

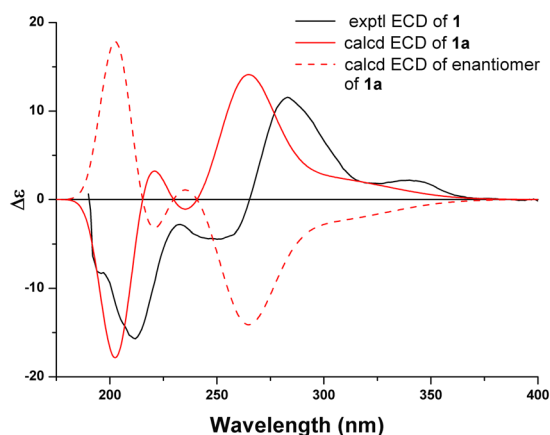


Figure 4. Experimental ECD spectrum of **1** and TDDFT calculated ECD spectra for **1a** (1*R*, 4*R*, 5*R*, 6*R*, 7*S*, 10*R*, 1'*R*) and enantiomer of **1a**.

(Fig. 6). The absolute configuration of **4** (1*R*, 4*R*, 5*S*, 9*S*) was determined to be the same as that of **17** by comparison of their ^{13}C NMR, NOESY, and ECD spectra, as well as TDDFT method (Fig. 9). *Psidium* terpenoids usually possess a C-1' coupling site on the 3,5-diformyl-benzyl phloroglucinol part^{6–10}. Psiguajadial D (**4**) with the C-14' coupling site represented the second example of this compound category, while the first example, guapsidial A (**17**), was reported recently from the same species¹¹.

Psiguajadial E (**5**) was assigned the molecular formula of $\text{C}_{30}\text{H}_{33}\text{O}_5$ by HR-ESI-MS, suggesting that it was an isomer of psiguajadial D (**13**)¹⁰. The 1D (Tables 3 and 4) and 2D NMR analysis (see Supplementary Fig. S1.1) revealed that **5** possessed the same gross structure as that of **13**, with main differences being observed at C-3 (δ_{C} 40.1 in **5**, 35.3 in **13**), C-5 (δ_{C} 80.1 in **5**, 85.2 in **13**), C-15 (δ_{C} 26.0 in **5**, 18.6 in **13**), and C-1' (δ_{C} 48.6 in **5**, 43.9 in **13**), indicating that the configuration of the coupling sites in **5** was varied. In the NOESY spectrum of **5** (Fig. 10), the key cross-peaks of H-9'(13')/H-5, H-10'(12')/H₃-14, and H-1'/H₃-15 suggested that H-1' and H₃-15 were α -oriented while H-5 was β -oriented. Thus, **5** was assigned as the C-1' epimer of **13**. This was further confirmed by comparison of the ECD spectra of **5** (see Supplementary S7.57) and **13**, which showed the reversed Cotton effects at 344 and 281 nm, as the Cotton effects arising from 3,5-diformyl-benzyl phloroglucinol moiety (UV λ_{max} at 340 and 279 nm) was dominated by the configuration of the chiral carbon C-1'. Thus, the structure of compound **5** was deduced as depicted.

Psiguajadial F (**6**) displayed a *quasi*-molecular ion peak at m/z 473.2353 [$\text{M} - \text{H}$]⁻ (calcd 473.2333) in HR-ESI-MS, in agreement with the molecular formula $\text{C}_{30}\text{H}_{34}\text{O}_5$. The 1D and 2D NMR analysis revealed that **6** shared the same gross structure with psiguajadial B⁹, a known caryolane-based *Psidium* monoterpene. Thus, the structural differences between the two compounds were attributable to the configurational variations on the coupling sites. The relative configuration of the caryolane moiety in **6** (C-1, C-4, C-8, and C-9) was assigned to be the same as those in psiguajadial B by NOESY analysis (Fig. 10) and comparison of their 1D NMR data. Consequently, the NOE correlations of H-3 α /H-5 and H-9 and H-1'/H-14b indicated that H-5 and H-1' were α - and β -oriented in **6**, respectively, which were reversed as in psiguajadial B. The absolute configuration of **6** was determined by comparison of its ECD spectrum (see Supplementary S7.58) with that of psiguajadial B, in which the reversed Cotton effects at 344 and 284 nm indicated that the configuration of C-1' in **6** was *S*. Thus, **6** was assigned as depicted.

Psiguajadial G (**7**) had the molecular formula $\text{C}_{30}\text{H}_{34}\text{O}_5$ as determined by HR-ESI-MS. Its 1D NMR data (Tables 3 and 4) were very similar to those of the synthesized caryophyllane-based meroterpenoid, compound

Position	1	2	3	4
1	34.6, C	32.9, C	138.2, C	53.2, CH
2	28.4, CH ₂	38.7, CH ₂	85.5, CH	22.0, CH ₂
3	33.5, CH ₂	44.3, CH	40.1, CH ₂	37.5, CH ₂
4	89.8, C	90.6, C	45.1, C	84.6, C
5	33.4, CH	40.8, CH	47.3, CH	33.2, CH
6	23.4, CH	27.0, CH	32.9, CH	33.5, CH ₂
7	44.3, CH	44.6, CH	25.1, CH	35.0, CH ₂
8	27.1, CH ₂	26.8, CH ₂	21.4, CH ₂	152.0, C
9	31.6, CH ₂	31.3, CH ₂	36.6, CH ₂	41.5, CH
10	30.5, CH	29.5, CH	136.0, C	36.4, CH ₂
11	33.6, CH	33.6, CH	18.8, C	33.7, C
12	19.6, CH ₃	19.9, CH ₃	28.2, CH ₃	22.1, CH ₃
13	20.2, CH ₃	20.0, CH ₃	15.9, CH ₃	30.2, CH ₃
14	19.0, CH ₃	18.8, CH ₃	22.1, CH ₃	20.4, CH ₃
15	42.2, CH ₂	23.8, CH ₃	22.9, CH ₃	110.3, CH ₂
1'	35.1, CH	35.2, CH	53.7, CH	200.3, C
2'	103.5, C	99.9, C	113.8, C	103.7, C
3'	165.8, C	163.4, C	167.4, C	162.2, C
4'	104.2, C	103.8, C	107.6, C	100.9, C
5'	168.5, C	168.7, C	167.8, C	167.3, C
6'	104.2, C	103.7, C	105.2, C	104.2, C
7'	169.8, C	169.7, C	170.0, C	168.9, C
8'	144.6, C	142.3, C	140.7, C	142.5, C
9'/13'	126.7, CH	127.3, CH	130.5, CH	127.7, CH
10'/12'	128.6, CH	128.5, CH	127.7, CH	126.7, CH
11'	126.3, CH	126.5, CH	126.4, CH	130.2, CH
14'	192.2, CH	192.1, CH	193.6, CH	24.3, CH ₂
15'	191.6, CH	191.4, CH	191.9, CH	192.1, CH

Table 2. ¹³C NMR (100 Hz) data of compounds **1–4** in CDCl₃ (δ in ppm).

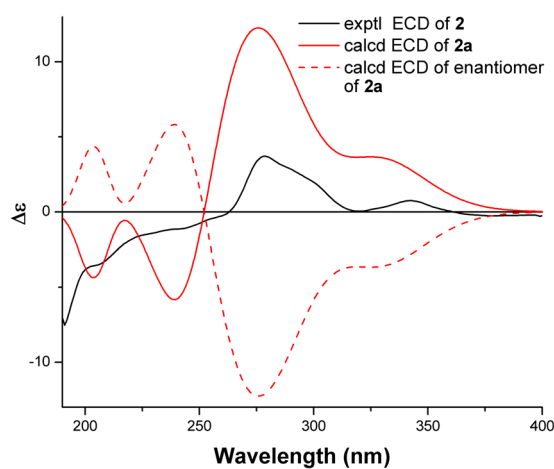


Figure 5. Experimental ECD spectrum of **2** and TDDFT calculated ECD spectra for **2a** (1*R*, 3*S*, 4*R*, 5*R*, 6*R*, 7*S*, 10*R*, 1'*R*) and enantiomer of **2a**.

20²⁷, which was isolated as a natural product for the first time in the current study and was given a trivial psiguajadial L. The structural difference between **7** and **20** was being due to the configuration of H-1', which was designated as α -orientation in **7** by NOE correlations of H₃-14/H-9' (13') and H-1'/H-5 and H-7 α (Fig. 11). Thus, psiguajadial G (**7**) was assigned as the C-1' epimer of **20**. The absolute configurations of psiguajadials G (**7**) and L (**20**) were established by analysis of their ECD spectra (see Supplementary S7.59 and S7.67), in which the Cotton effects around at 345 nm (positive for **7** and negative for **20**) and 284 nm (positive for **7** and negative for **20**) indicated that the C-1' configuration of **7** and **20** were *R* and *S*, respectively. These assignments were in agreement with the ECD tendencies of those for guajadial (**19**) and psidial A (**18**)^{9,27}, respectively.

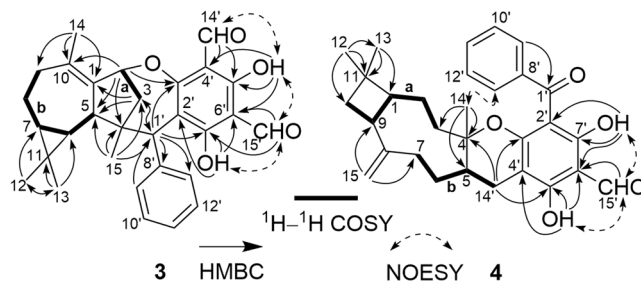


Figure 6. Selected ^1H - ^1H COSY, HMBC, and NOESY correlations of **3** and **4**.

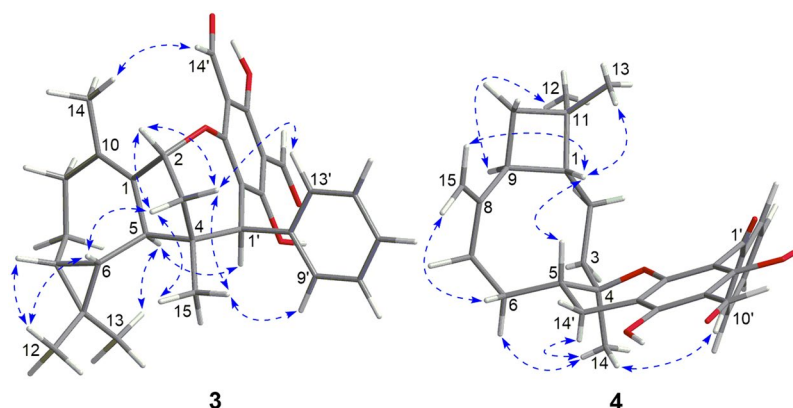


Figure 7. Selected NOESY correlations of **3** and **4**.

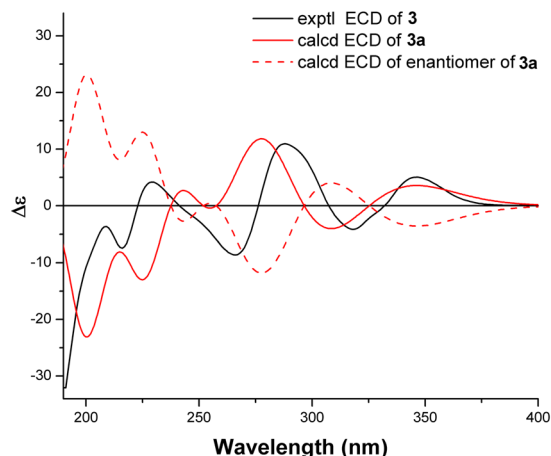


Figure 8. Experimental ECD spectrum of **3** and TDDFT calculated ECD spectra for **3a** (2*R*, 4*S*, 5*R*, 6*R*, 7*R*, 1'*R*) and enantiomer of **3a**.

Psiguajadials **H** (**8**) and **I** (**9**) had the identical molecular formula $\text{C}_{30}\text{H}_{34}\text{O}_5$ on the basis of their HR-ESI-MS data. Analysis of their 1D and 2D NMR data indicated that both compounds had the same gross structure as the known cadinane-based *Pisudium* meroterpenoids guajadials **C** (**21**) and **D** (**22**)³⁴, a pair of C-1' epimers also isolated in the current study. The relative configurations of the cadinane moiety (C-1, C-7, and C-10) in **8** and **9** were established as the same as those in **21** and **22** based on the NOESY analysis and comparison of their 1D NMR data. Thus, the remaining two chiral centers (C-4 and C-1') formed by the spiro ring junction suggested that **8**, **9**, **21**, and **22** were four stereoisomers. Detailed NOESY analysis of **8** and **9** (Fig. 11) indicated that they had the same configuration at the spirocenter (C-4–C-15 bond α -oriented) but different configuration at C-1' (H-1' β in **8** and H-1' α in **9**). Thus, compounds **8** and **9** were also a pair of C-1' epimers. The absolute configurations of **8** and **9** were established by analysis of their ECD spectra (see Supplementary S7.60 and S7.61), in which the Cotton effects at 344 nm (negative for **8** and positive for **9**) and 284 nm (negative for **8** and positive for **9**) indicated that

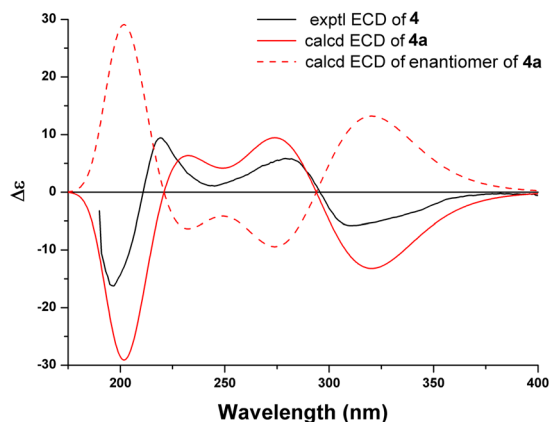


Figure 9. Experimental ECD spectrum of **4** and TDDFT calculated ECD spectra for **4a** (1*R*, 4*R*, 5*S*, 9*S*) and enantiomer of **4a**.

Position	5	6	7	8	9	10
1	4.90, dd (12.3, 3.5)	1.75, m	1.57, m	2.36, m	2.35, m	2.21, m
2	α 1.55, m; β 1.24, m	α 1.64, m; β 1.31, m	β 1.51, m; α 1.32, m	a 1.50, m; b 1.34, m	β 1.85, m; α 1.44, m	β 1.53, m; α 1.21, m
3	a 2.01, m; b 1.80, m	α 1.95, m; β 1.80, m	a 2.12, dd (15.7, 10.0); b 1.76, m	1.82, m	β 1.79, m; α 1.67, m	1.89, m
5	4.45, d (7.1)	2.10, m	2.51, m	5.31, s	5.58, s	5.67, d (1.6)
6	0.93, t (7.8)	α 1.91, m; β 1.72, m	a 1.89, m; b 1.28, m	—	—	—
7	0.57, m	β 1.46, m; α 1.38, m	β 2.52, m; α 2.31, dd (13.6, 9.9)	1.49, m	1.62, m	1.67, m
8	α 1.90, m; β 1.00, m	—	—	α 1.80, m; β 1.61, m	α 1.70, m; β 1.61, m	1.65, m
9	β 1.95, m; α 1.88, m	2.16, m	2.63, dd (18.1, 9.1)	β 1.78, m; α 1.30, m	β 1.85, m; α 1.33, m	β 1.67, m; α 1.33, m
10	—	α 1.51, m; β 1.32, m	1.73, m	1.94, m	1.94, m	1.83, m
11	—	—	—	1.81, m	1.81, m	1.74, m
12	α 1.17, s	α 0.97, s	α 0.96, s	0.78, d (6.5)	0.65, d (6.6)	0.75, d (6.1)
13	β 1.23, s	β 0.99, s	β 0.99, s	0.90, d (6.4)	0.89, d (6.9)	0.91, d (6.0)
14	1.08, s	a 1.59, d (12.8); b 1.39, d (12.8)	1.05, s	0.82, d (7.0)	0.85, d (7.2)	0.86, d (6.7)
15	1.13, s	0.84, s	4.89, s 4.81, s	β 2.23, dd (14.2, 7.0); α 2.13, dd (14.2, 9.4)	α 2.32, dd (14.0, 6.9); β 2.02, dd (14.0, 9.8)	1.34, s
1'	3.78, s	3.76, d (8.1)	4.34, d (6.1)	4.08, t (8.1)	4.17, t (8.5)	3.49, d (11.6)
9'/13'	7.33, m	7.13, d (7.0)	7.11, d (7.4)	7.15, d (7.3)	7.16, d (7.5)	7.13, d (7.0)
10'/12'	7.25, m	7.26, t (7.0)	7.26, m	7.27, t (7.0)	7.29, t (7.0)	7.28, t (7.0)
11'	7.15, t (7.0)	7.29, t (7.0)	7.22, m	7.20, t (7.0)	7.21, t (7.0)	7.22, t (7.0)
14'	10.19, s	10.09, s	10.10, s	10.04, s	10.04, s	10.04, s
15'	10.07, s	10.08, s	10.15, s	10.13, s	10.13, s	10.08, s
5'-OH	13.74, s	13.48, s	13.63, s	13.53, s	13.51, s	13.54, s
7'-OH	13.05, s	13.11, s	13.20, s	13.18, s	13.18, s	13.07, s

Table 3. ^1H NMR (400 Hz) data of compounds **5–10** in CDCl_3 (δ in ppm, *J* in Hz).

the C-1' configuration of **8** and **9** were *S* and *R*, respectively. These assignments were in agreement with the ECD tendencies of those for **21** and **22**, respectively.

Psiguajadial **10** had the molecular formula $\text{C}_{30}\text{H}_{34}\text{O}_5$ as determined on the basis of HR-ESI-MS and NMR data. The 1D and 2D NMR analysis revealed that **10** shared the same gross structure with those of guajadials **E** (**23**) and **F** (**24**)³⁴, a pair of C-1' epimers of cadinane-based *Psidium* meroterpenoid, indicating that they were stereoisomers with configurational variations occurring at the coupling sites (C-1', C-3, and C-4). The relative configuration of **10** was established by NOESY experiment and analysis of its coupling constant. The NOE correlations of H-1/H-3, H-9 β , and H-11 and H-3/H-9' (13'), and H-2 β indicated that these protons and the benzene ring were cofacial and were arbitrarily assigned as β -orientated. Thus, the NOE correlations of H₃-15/H-1', H-2 α ,

Position	5	6	7	8	9	10
1	127.1, CH	44.3, CH	57.7, CH	36.1, CH	36.5, CH	38.4, CH
2	24.3, CH ₂	20.5, CH ₂	23.2, CH ₂	22.9, CH ₂	22.8, CH ₂	26.1, CH ₂
3	40.1, CH ₂	37.8, CH ₂	42.3, CH ₂	30.6, CH ₂	33.7, CH ₂	45.9, CH
4	40.9, C	85.0, C	86.1, C	78.9, C	78.9, C	80.2, C
5	80.1, CH	43.4, CH	39.0, CH	125.5, CH	122.8, CH	127.8, CH
6	28.5, CH	23.3, CH ₂	27.7, CH ₂	145.5, C	146.9, C	141.9, C
7	32.8, CH	32.6, CH ₂	36.1, CH ₂	51.1, CH	51.2, CH	50.0, CH
8	23.3, CH ₂	33.3, C	154.2, C	22.7, CH ₂	22.7, CH ₂	22.3, CH ₂
9	37.7, CH ₂	38.4, CH	42.6, CH	29.0, CH ₂	29.0, CH ₂	28.7, CH ₂
10	131.3, C	35.5, CH ₂	37.6, CH ₂	34.9, CH	34.9, CH	32.6, CH
11	19.4, C	34.7, C	33.5, C	26.5, CH	26.6, CH	26.6, CH
12	30.5, CH ₃	20.9, CH ₃	22.6, CH ₃	21.4, CH ₃	21.3, CH ₃	21.8, CH ₃
13	19.9, CH ₃	30.6, CH ₃	29.6, CH ₃	21.1, CH ₃	21.2, CH ₃	21.2, CH ₃
14	18.0, CH ₃	41.9, CH ₂	22.9, CH ₃	14.4, CH ₃	14.3, CH ₃	13.9, CH ₃
15	26.0, CH ₃	26.5, CH ₃	110.3, CH ₂	42.3, CH ₂	42.8, CH ₂	19.7, CH ₃
1'	48.6, CH	37.9, CH	35.8, CH	34.3, CH	34.3, CH	41.0, CH
2'	105.7, C	103.2, C	103.7, C	102.8, C	103.3, C	105.3, C
3'	163.0, C	162.8, C	164.2, C	164.5, C	164.7, C	164.1, C
4'	103.6, C	104.0, C	103.8, C	104.5, C	104.6, C	104.5, C
5'	168.6, C	168.4, C	168.75, C	168.6, C	168.5, C	168.5, C
6'	104.0, C	104.0, C	103.6, C	104.0, C	104.1, C	104.2, C
7'	168.8, C	169.6, C	168.83, C	169.7, C	169.7, C	169.7, C
8'	142.9, C	145.0, C	139.2, C	144.3, C	144.6, C	143.3, C
9'/13'	128.6, CH	127.9, CH	130.2, CH	126.9, CH	126.8, CH	127.8, CH
10'/12'	126.9, CH	128.3, CH	127.8, CH	128.4, CH	128.5, CH	128.2, CH
11'	126.7, CH	126.3, CH	126.7, CH	126.1, CH	126.2, CH	126.3, CH
14'	192.7, CH	191.5, CH	192.2, CH	192.3, CH	192.2, CH	192.4, CH
15'	191.4, CH	192.2, CH	192.5, CH	191.5, CH	191.6, CH	191.5, CH

Table 4. ¹³C NMR (100 Hz) data of compounds **5**–**10** in CDCl₃ (δ in ppm).

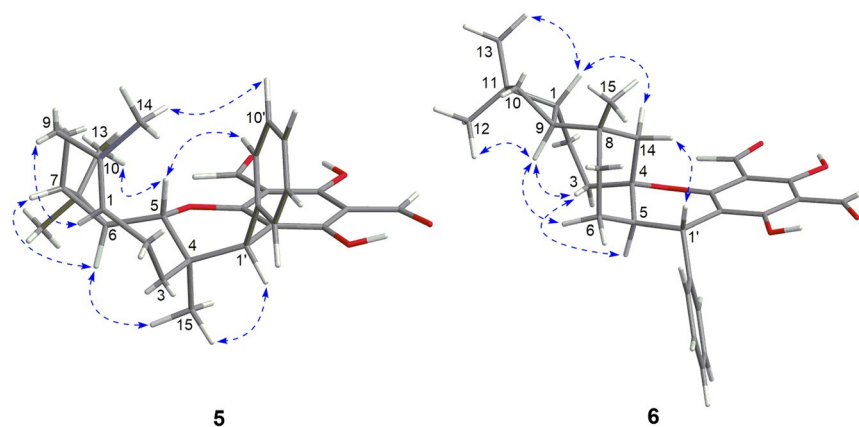


Figure 10. Selected NOESY correlations of **5** and **6**.

and H₃-14 (Fig. 11), assigned these protons or methyl group in α -orientation. The *trans*-relationship of H-1' and H-3 were further confirmed by the large coupling constant of H-1' ($J = 11.6$ Hz). Thus, **10** was established as a C-3 epimer of **24**, with a *trans*-fused dihydropyran ring. The *R*-configuration of C-1' in **10** was established by the Cotton effects at 346 (positive) and 278 nm (positive) in its ECD spectrum (see Supplementary S7.62), which showed the similar tendency to those of **24**.

Psiguajadial K (**11**) had a molecular formula of C₂₅H₂₅O₅ as determined by its HR-ESI-MS. The 1D (Table 5) and 2D NMR analysis (Fig. 12) revealed that **11** possessed the same gross structure as that of guajal A (**26**)¹⁰, indicating that they were stereoisomers with configurational variations occurring at the coupling sites. In the NOESY spectrum, the correlations of H-2/H-7 β and H-1'/H-6 β and H-7 α (Fig. 12) indicated that C-1–C-7 bond was β -oriented at the spirocenter while H-1' was α -oriented on the pyran ring. Thus, **11** was established as the

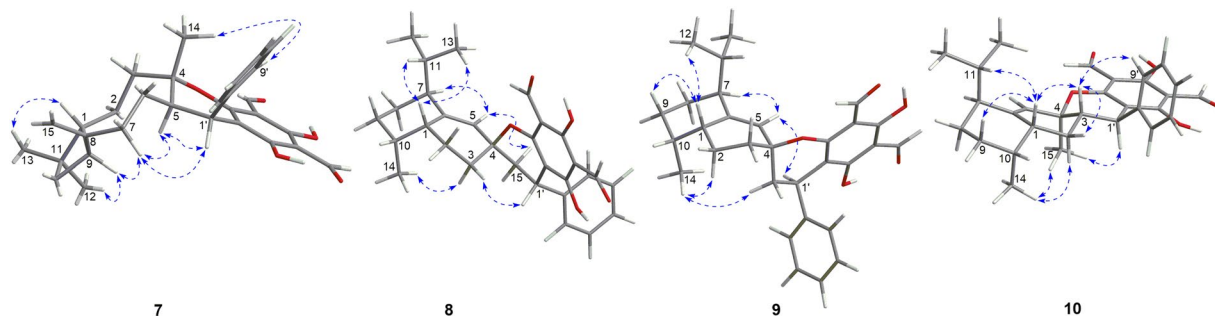


Figure 11. Selected NOESY correlations of 7–10.

Position	11	
	δ_{H} , multi. (<i>J</i> in Hz)	δ_{C} , type
1	—	88.7, C
2	1.06, dd (7.8, 3.5)	30.0, CH
3	α 0.81, dd (5.2, 3.5); β 0.41, dd (7.8, 5.2)	11.6, CH ₂
4	—	33.6, C
5	1.71, m	25.1, CH ₂
6	β 1.84, m; α 1.50, m	32.1, CH ₂
7	β 2.30, dd (14.3, 7.4); α 2.23, ddd (14.3, 7.6, 1.0)	40.5, CH ₂
8	1.21, t (6.9)	32.1, CH
9	0.76, d (6.8)	19.3, CH ₃
10	0.73, d (6.9)	19.3, CH ₃
1'	4.15, t (7.5)	34.3, CH
2'	—	102.6, C
3'	—	165.3, C
4'	—	104.4, C
5'	—	168.5, C
6'	—	104.0, C
7'	—	169.8, C
8'	—	144.2, C
9'/13'	7.18, d (7.0)	127.0, CH
10'/12'	7.28, t (7.0)	128.5, CH
11'	7.20, t (7.0)	126.3, CH
14'	10.13, s	191.6, CH
15'	10.12, s	192.4, CH
5'-OH	13.56, s	
7'-OH	13.19, s	

Table 5. ¹H (400 Hz) and ¹³C NMR (100 Hz) data of compound **11** in CDCl₃ (δ in ppm).

C-1' epimer of guajadial A. This was further confirmed by the ECD spectrum of **11**, which showed the reversed Cotton effects at 341 (positive) and 278 nm (positive) as compared to those of **26**.

The spectroscopic data of compound **12** was identical to guajavadiol C, a new skeleton of bicyclogermacrene-based *Psidium* meroterpenoid recently isolated from the same plant by Qin *et al.*³⁵. However, after careful analysis of its NMR data, we found the configuration of guajavadiol C was incorrect (see Supplementary Fig. S1.2). The *cis*-relationship of H-5 and H-1' was assigned by the author only based on the NOE correlation of H-5/H-1'. In fact, on a six-membered ring both *cis* and *trans* adjacent protons could generate NOE correlations. In this case, the *trans*-relationship of H₃-15 and H-5 was firstly assigned by the NOE correlations of H-5/H₃-13 and H-3 β , and H-6/H₃-15 (see Supplementary Fig. S1.2). Then the NOE correlations of H-9'(13')/H-3 β further assigned the benzene group in β -orientation. Thus, H-1' was α -oriented and in the *trans*-position of H-5. In addition, the configuration of $\Delta^{1(10)}$ was revised as *E* by the observed NOE correlation of H-1/H-9 β . The absolute configuration of **12** was established as 4*S*, 5*R*, 6*R*, 7*R*, 1'*S* by comparison of its experimental ECD spectrum with those of calculated for its isomers (see Supplementary Fig. S1.3).

(\pm)-Guajadial B⁸, a racemic *Psidium* meroterpenoid previously isolated from the same plant, was chirally separated in the current study to afford a pair of enantiomers, (–)-guajadial B (**14**) ($[\alpha]_{\text{D}}^{26} -30.0$) and (+)-guajadial B (**15**) ($[\alpha]_{\text{D}}^{26} +30.0$). The absolute configurations of **14** (3*R*, 4*S*, 1'*S*) and **15** (3*S*, 4*R*, 1'*R*) were established by

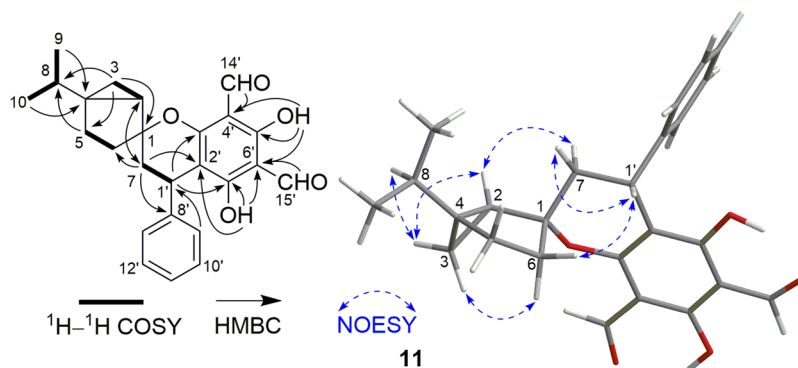


Figure 12. Selected ^1H - ^1H COSY, HMBC, and NOESY correlations of **11**.

analysis of their ECD spectra (see Supplementary S7.65 and S7.66), in which the Cotton effects at 348 and 290 nm were correlated with the configuration of C-1' as described for the aforementioned *Psidium* meroterpenoids.

The known compounds psiguajadial D (**13**)¹⁰, psiguajadial A (**16**)⁹, guapsidial A (**17**)¹¹, psidial A (**18**), guajadial (**19**)^{9,27}, psiguajadial L (**20**)²⁷, guajadials C-F (**21**-**24**)³⁴, guajavadial A (**25**)³⁵, guajadial A (**26**)¹⁰, guajadial B (**27**)¹¹, and guajadial C (**28**)¹¹ were identified by comparison of their NMR (see Supplementary Tables S2.23-S2.7) and optical rotation data with those in the literature. In addition, the absolute configurations of psiguajadial L (**20**) and guajadials C-F (**21**-**24**) were established for the first time based on ECD analysis (see Supplementary S7.67-S7.71).

The biosynthesis of *Psidium* meroterpenoids was previously hypothesized to occur *via* hetero-Diels-Alder reactions or a series of electrophilic addition reactions between the mono- or sesquiterpenoid precursors and the key intermediate 3,5-dimethyl-2,4,6-trihydroxybenzophenone^{6, 10, 11, 36}. The hetero-Diels-Alder pathway was supported by the biomimetic synthesis of (\pm)-guajadial B, psidial A (**18**), guajadial (**19**), psiguajadial L (**20**), and psiguajadial D (**13**)^{8, 25, 27}. Thus, the biosynthetic pathways of the new skeleton compounds (**1** and **2**) in this study were proposed based on the hetero-Diels-Alder reaction as shown in Fig. 13. 3,5-Dimethyl-2,4,6-trihydroxybenzophenone, which has been previously isolated from the same plant^{10, 37}, is presumed to be the biogenetic precursor of the benzyl phloroglucinol intermediates **i**⁹. Dehydration of **i** further produced the *O*-quinone methide intermediate **ii**. β -Cubebene and α -cubebene, which have been reported to be present in the same species^{10, 38, 39}, are deemed to be the sesquiterpenoid precursors. Reaction of the terpenoid precursors with **ii** *via* hetero-Diels-Alder reactions would afford **1** and **2**.

Compounds **1**-**28** were tested for their inhibitory activities against PDE4D2. Rolipram, a well-known PDE4 inhibitor, was used as the positive control (IC_{50} $0.62 \pm 0.03 \mu\text{M}$). Most of compounds (**1**-**13** and **16**-**26**) exhibited moderate inhibitory activities with IC_{50} values in the range of 1.34-7.26 μM (Table 6), which may explain the inhibitory activity of the selected fraction and the anti-inflammatory usage of *P. guajava* in traditional medicine.

Psidium meroterpenoids are a small group of natural products characterized by a 3,5-diformyl-benzyl phloroglucinol moiety coupled with a mono- or sesquiterpenoid unit. In the current study, bioassay-guided fractionation of the ethanolic extract of the leaves of *Psidium guajava* led to the isolation of 28 *Psidium* meroterpenoids, including 11 new ones (**1**-**11**). Compounds **1** and **2** represent two unprecedented skeletons with the presence of cubebene moiety in this compound class reported for the first time. Compound **3** represents the first example of *Psidium* meroterpenoid coupling *via* an oxepane ring, and **4** was the second example featuring the C-14' coupling site. Compounds **1**-**13** and **16**-**26** exhibited moderate inhibitory activities against phosphodiesterase-4 (PDE4), with IC_{50} values in the range of 1.34-7.26 μM , suggesting that this compound class represents a new class of PDE4 inhibitors, which may serve as new structural motifs for designing new PDE4 inhibitors. Investigations of their mechanism of action and selectivity *versus* other PDEs are ongoing.

Methods

General. Optical rotations were determined on a Perkin-Elmer 341 polarimeter at 20 °C. UV spectra were performed on a Shimadzu UV-2450 spectrophotometer, and ECD spectra were performed on an Applied Photophysics Chirascan spectrometer. Infrared spectra (IR) were measured on a Bruker Tensor 37 infrared spectrophotometer. NMR experiments were carried out on a Bruker AM-400 spectrometer at the temperature thermostatically controlled at 25 °C. Exact mass measurements and molecular formulas were obtained from ESIMS and HR-ESI-MS using a Finnigan LCQ Deca and a Thermo Scientific LTQ Orbitrap XL spectrometers, respectively. Semi-preparative reversed-phase (RP) HPLC was performed with a YMC-pack ODS-A column (10 \times 250 mm, S-5 μm) or a Phenomenex Lux cellulose-2 chiral column (10 \times 250 mm, 5 μm) under Shimadzu LC-20 AT equipped with a SPD-M20A PDA detector. Column chromatography (CC) was performed on RP-C₁₈ silica gel (S-50 μm , 12 nm, YMC Co., Ltd.), MCI gel (CHP20P, 75-150 μm , Mitsubishi Chemical Industries Ltd.), Sephadex LH-20 gel (Amersham Biosciences), and silica gel (300-400 mesh, Qingdao Haiyang Chemical Co., Ltd.). For RP-HPLC and CC, the analytical grade solvents (Guangzhou Chemical Reagents Company, Ltd.) were employed.

Plant material. *P. guajava* were collected in Guangzhou, Guangdong Province, China, in August 2014. The plant was identified by Dr. You-Kai Xu, Xishuangbanna Tropical Botanical Garden, Chinese Academy of Sciences,

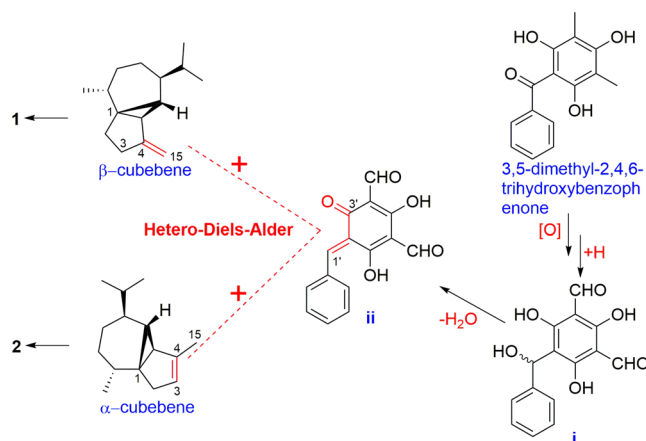


Figure 13. A plausible biosynthetic pathway of **1** and **2**.

Compound	IC ₅₀ (μ M)	Compound	IC ₅₀ (μ M)	Compound	IC ₅₀ (μ M)
1	3.11 \pm 0.10	11	3.68 \pm 0.27	21	2.28 \pm 0.11
2	5.03 \pm 0.33	12	4.33 \pm 0.21	22	1.93 \pm 0.11
3	4.50 \pm 0.28	13	3.42 \pm 0.21	23	2.73 \pm 0.15
4	4.14 \pm 0.26	14	>50	24	2.67 \pm 0.17
5	3.25 \pm 0.20	15	>50	25	2.01 \pm 0.07
6	2.63 \pm 0.13	16	7.26 \pm 0.41	26	2.70 \pm 0.15
7	1.34 \pm 0.33	17	5.61 \pm 0.51	27	>50
8	1.81 \pm 0.09	18	1.60 \pm 0.09	28	17.09 \pm 0.96
9	2.51 \pm 0.17	19	1.62 \pm 0.08	rolipram^a	0.62 \pm 0.03
10	2.53 \pm 0.33	20	1.37 \pm 0.07		

Table 6. IC₅₀ Values of compounds against PDE4D2. ^aPositive control.

and voucher specimens (FSL201408) have been stored at the School of Pharmaceutical Sciences, Sun Yat-sen University.

Extraction and isolation. Sequential extraction was carried out on 6.0 kg of the air-dried leaves of *P. guajava* with 95% EtOH immersion (10 L \times 4) at rt. After evaporating the solvent, the residue (320 g) was suspended in H₂O (1.5 L) and extracted with EtOAc (1.5 L \times 3) and *n*-BuOH (1.5 L \times 3), respectively. The EtOAc partition (165 g) was chromatographed over MCI gel CC (MeOH-H₂O, 10% \rightarrow 100%) to give seven sub-fractions (A–G).

Each fraction was subjected to CC over RP-C₁₈ column, silica gel, and Sephadex LH-20 and then further purified by semipreparative HPLC with a YMC-pack ODS-A column or a Phenomenex Lux chiral column to yield pure compounds. Compounds **11** (2 mg), **13** (256 mg), **19** (532 mg), **20** (222 mg), and **23** (433 mg) were obtained from Fr. B. Fr. D gave compounds **14** (23 mg) and **15** (24 mg). Fr. E afforded compounds **4** (14 mg), **5** (11 mg), **7** (14 mg), **8** (49 mg), **10** (17 mg), **17** (6 mg), **21** (113 mg), **22** (17 mg), **24** (72 mg), **26** (1 mg), and **28** (17 mg). Compounds **1** (14 mg), **2** (19 mg), **3** (5 mg), **6** (5 mg), **11** (9 mg), **12** (13 mg), **16** (8 mg), **18** (269 mg), **25** (26 mg), and **27** (8 mg) were obtained from Fr. F. The details on isolation of these compounds are provided in Supplementary S3.1.

Psiguajadial A (1). Colourless oil; $[\alpha]_D^{26} + 22$ (c 0.3, CHCl₃); UV (MeCN) λ_{\max} (log ϵ) 280 (4.5) nm; ECD (c 1.1×10^{-4} M, MeCN); λ_{\max} ($\Delta\epsilon$) 340 (+2.2), 283 (+11.6), 250 (−4.5), 212 (−15.7) nm; IR (KBr) ν_{\max} 3448, 2957, 2924, 2851, 1633, 1439, 1302, 1181, 773 cm^{−1}; ¹H and ¹³C NMR data, see Tables 1 and 2; (−) MS-ESI m/z 473.3 [M − H][−]; (−) HR-MS-ESI m/z 473.2304 [M − H][−] (calcd for C₃₀H₃₃O₅, 473.2333).

Psiguajadial B (2). Colourless oil; $[\alpha]_D^{26} + 7.1$ (c 0.5, CHCl₃); UV (MeCN) λ_{\max} (log ϵ) 197 (4.4), 278 (4.6), 343 (3.6) nm; ECD (c 4.2×10^{-4} M, MeCN) λ_{\max} ($\Delta\epsilon$) 342 (+0.8), 279 (+3.7), 191 (−7.5) nm; IR (KBr) ν_{\max} 3448, 2955, 2925, 2869, 1633, 1443, 1381, 1305, 1179 cm^{−1}; ¹H and ¹³C NMR data, see Tables 1 and 2; (+) MS-ESI m/z 475.3 [M + H]⁺; (+) HR-MS-ESI m/z 475.2475 [M + H]⁺ (calcd for C₃₀H₃₅O₅, 475.2479).

Psiguajadial C (3). Colourless oil; $[\alpha]_D^{26} + 76.6$ (c 0.2, CHCl₃); UV (MeCN) λ_{\max} (log ϵ) 198 (4.5), 275 (4.5), 347 (3.6) nm; ECD (c 4.2×10^{-4} M, MeCN) λ_{\max} ($\Delta\epsilon$) 346 (+5.1), 318 (−4.2), 288 (+11.0), 266 (−8.6), 229 (+4.2), 216 (−7.4), 191 (−32.1) nm; IR (KBr) ν_{\max} 3447, 2958, 2922, 2872, 1634, 1602, 1445, 1379, 1306, 1130 cm^{−1}; ¹H and ¹³C NMR data, see Tables 1 and 2; (−) MS-ESI m/z 471.2 [M − H][−]; (−) HR-MS-ESI m/z 471.2191 [M − H][−] (calcd for C₃₀H₃₁O₅, 471.2177).

Psiguajadial D (4). Colourless oil; $[\alpha]_D^{26} - 149$ (c 0.2, CHCl₃); UV (MeCN) λ_{\max} (log ϵ) 199 (4.5), 285 (4.5) nm; ECD (c 2.1×10^{-4} M, MeCN) λ_{\max} ($\Delta\epsilon$) 308 (−5.7), 282 (+5.8), 218 (+9.2), 196 (−16.2) nm; IR (KBr) ν_{\max} 3453,

2950, 2924, 2857, 1630, 1605, 1425, 1317, 1287, 697 cm^{-1} ; ^1H and ^{13}C NMR data, see Tables 1 and 2; (–) MS-ESI m/z 473.3 $[\text{M} - \text{H}]^-$; (–) HR-MS-ESI m/z 473.2319 $[\text{M} - \text{H}]^-$ (calcd for $\text{C}_{30}\text{H}_{33}\text{O}_5$, 473.2333).

Psiguajadial E (5). Colourless oil; $[\alpha]_D^{26} -105.4$ (c 0.3, CHCl_3); UV (MeCN) λ_{max} ($\log \epsilon$) 199 (4.6), 279 (4.6), 340 (3.7) nm; ECD (c 4.2×10^{-4} M, MeCN) λ_{max} ($\Delta\epsilon$) 344 (+0.7), 304 (+1.8), 281 (+0.9), 265 (–3.6), 221 (–7.1), 190 (–21.3) nm; IR (KBr) ν_{max} 3437, 2955, 2922, 2854, 1628, 1439, 1382, 1300, 1267, 1181 cm^{-1} ; ^1H and ^{13}C NMR data, see Tables 3 and 4; (–) MS-ESI m/z 473.3 $[\text{M} - \text{H}]^-$; (–) HR-MS-ESI m/z 473.2297 $[\text{M} - \text{H}]^-$ (calcd for $\text{C}_{30}\text{H}_{33}\text{O}_5$, 473.2333).

Psiguajadial F (6). Colourless oil; $[\alpha]_D^{26} -50.3$ (c 0.2, CHCl_3); UV (MeCN) λ_{max} ($\log \epsilon$) 198 (4.4), 278 (4.5), 343 (3.5) nm; ECD (c 4.2×10^{-4} M, MeCN) λ_{max} ($\Delta\epsilon$) 344 (–2.5), 284 (–13.5), 247 (+3.6), 206 (+20.0), 190 (+12.8) nm; IR (KBr) ν_{max} 3432, 2955, 2922, 2870, 1634, 1443, 1383, 1306, 1181 cm^{-1} ; ^1H and ^{13}C NMR data, see Tables 3 and 4; (–) MS-ESI m/z 473.2 $[\text{M} - \text{H}]^-$; (–) HR-MS-ESI m/z 473.2353 $[\text{M} - \text{H}]^-$ (calcd for $\text{C}_{30}\text{H}_{33}\text{O}_5$, 473.2333).

Psiguajadial G (7). Colourless oil; $[\alpha]_D^{26} -61.7$ (c 0.2, CHCl_3); UV (MeCN) λ_{max} ($\log \epsilon$) 199 (4.6), 278 (4.6), 340 (3.7) nm; ECD (c 4.2×10^{-4} M, MeCN) λ_{max} ($\Delta\epsilon$) 345 (+1.1), 279 (+6.0), 254 (–2.1), 201 (–12.8), 190 (–11.5) nm; IR (KBr) ν_{max} 3466, 2952, 2925, 2856, 1630, 1439, 1382, 1302, 1182 cm^{-1} ; ^1H and ^{13}C NMR data, see Tables 3 and 4; (–) MS-ESI m/z 473.3 $[\text{M} - \text{H}]^-$; (–) HR-MS-ESI m/z 473.2296 $[\text{M} - \text{H}]^-$ (calcd for $\text{C}_{30}\text{H}_{33}\text{O}_5$, 473.2333).

Psiguajadial H (8). Colourless oil; $[\alpha]_D^{26} -6.3$ (c 0.4, CHCl_3); UV (MeCN) λ_{max} ($\log \epsilon$) 198 (4.5), 278 (4.5), 342 (3.6) nm; ECD (c 4.2×10^{-4} M, MeCN) λ_{max} ($\Delta\epsilon$) 344 (–1.5), 328 (–1.5), 284 (–6.0), 259 (+4.1), 216 (+17.8), 191 (+10.2) nm; IR (KBr) ν_{max} 3431, 2956, 2924, 2871, 1635, 1441, 1381, 1303, 1182 cm^{-1} ; ^1H and ^{13}C NMR data, see Tables 4 and 5; (–) MS-ESI m/z 473.2 $[\text{M} - \text{H}]^-$; (–) HR-MS-ESI m/z 473.2351 $[\text{M} - \text{H}]^-$ (calcd for $\text{C}_{30}\text{H}_{33}\text{O}_5$, 473.2333).

Psiguajadial I (9). Colourless oil; $[\alpha]_D^{26} -37.8$ (c 0.4, CHCl_3); UV (MeCN) λ_{max} ($\log \epsilon$) 197 (4.5), 278 (4.5), 342 (3.6) nm; ECD (c 4.2×10^{-4} M, MeCN) λ_{max} ($\Delta\epsilon$) 344 (+2.3), 284 (+7.8), 257 (–7.1), 215 (–23.2), 190 (–19.8) nm; IR (KBr) ν_{max} 3441, 2956, 2923, 2871, 1634, 1441, 1380, 1304, 1181 cm^{-1} ; ^1H and ^{13}C NMR data, see Tables 3 and 4; (+) MS-ESI m/z 475.3 $[\text{M} + \text{H}]^+$, 497.2 $[\text{M} + \text{Na}]^+$; (+) HR-MS-ESI m/z 475.2479 $[\text{M} + \text{H}]^+$ (calcd for $\text{C}_{30}\text{H}_{35}\text{O}_5$, 475.2479).

Psiguajadial J (10). Colourless oil; $[\alpha]_D^{26} +124.1$ (c 0.6, CHCl_3); UV (MeCN) λ_{max} ($\log \epsilon$) 198 (4.5), 278 (4.6), 342 (3.6) nm; ECD (c 4.2×10^{-4} M, MeCN) λ_{max} ($\Delta\epsilon$) 346 (+1.0), 278 (+14.5), 246 (–2.4), 226 (+2.4), 218 (–1.3), 212 (+1.4), 191 (–21.6) nm; IR (KBr) ν_{max} 3429, 2957, 2925, 2872, 1364, 1141, 1380, 1304, 1263, 1185, 1155 cm^{-1} ; ^1H and ^{13}C NMR data, see Tables 3 and 4; (+) MS-ESI m/z 475.3 $[\text{M} + \text{H}]^+$, 497.2 $[\text{M} + \text{Na}]^+$; (+) HR-MS-ESI m/z 475.2477 $[\text{M} + \text{H}]^+$ (calcd for $\text{C}_{30}\text{H}_{35}\text{O}_5$, 475.2479).

Psiguajadial K (11). Colourless oil; $[\alpha]_D^{26} +147.6$ (c 0.1, CHCl_3); UV (MeCN) λ_{max} ($\log \epsilon$) 230 (4.1), 280 (4.5), 342 (3.5) nm; ECD (c 1.2×10^{-4} M, MeCN) λ_{max} ($\Delta\epsilon$) 341 (+2.1), 278 (+20.6), 250 (–4.0), 230 (+2.3), 213 (–16.4), 190 (+17.6) nm; IR (KBr) ν_{max} 3446, 2957, 2924, 2851, 1635, 1559, 1440, 1381, 1302, 1182 cm^{-1} ; ^1H and ^{13}C NMR data, see Table 5; (–) MS-ESI m/z 405.4 $[\text{M} - \text{H}]^-$; (–) HR-MS-ESI m/z 405.1688 $[\text{M} - \text{H}]^-$ (calcd for $\text{C}_{25}\text{H}_{25}\text{O}_5$, 405.1707).

Guajavadial C (12). Colourless oil; $[\alpha]_D^{26} -44.7$ (c 0.4, CHCl_3); UV (MeCN) λ_{max} ($\log \epsilon$) 197 (4.5), 275 (4.5), 346 (3.5) nm; ECD (c 4.2×10^{-4} M, MeCN) λ_{max} ($\Delta\epsilon$) 346 (–1.9), 314 (+3.4), 285 (–13.2), 251 (+3.0), 218 (+1.2), 209 (–0.3), 192 (+10.6) nm; IR (KBr) ν_{max} 3429, 2956, 2923, 2870, 1638, 1445, 1380, 1305, 1176 cm^{-1} ; ^1H and ^{13}C NMR data, see Supplementary Table S2.3; (–) MS-ESI m/z 473.2 $[\text{M} - \text{H}]^-$; (–) HR-MS-ESI m/z 473.2356 $[\text{M} - \text{H}]^-$ (calcd for $\text{C}_{30}\text{H}_{33}\text{O}_5$, 473.2333).

(–) **Guajadial B (14).** $[\alpha]_D^{26} -30.0$ (c 0.1, CHCl_3); ECD (c 5.5×10^{-4} M, MeCN) λ_{max} ($\Delta\epsilon$) 348 (–2.6), 334 (–0.5), 290 (–24.3), 260 (+7.2), 228 (–7.0), 216 (+25.6), 197 (+31.3) nm.

(+) **Guajadial B (15).** $[\alpha]_D^{26} +30.0$ (c 0.1, CHCl_3); ECD (c 3.6×10^{-4} M, MeCN) λ_{max} ($\Delta\epsilon$) 348 (+3.7), 334 (+0.4), 289 (+35.1), 261 (–10.5), 228 (+12.2), 217 (–33.5), 190 (+25.6) nm.

Psiguajadial N (20). ECD (c 4.6×10^{-4} M, MeCN) λ_{max} ($\Delta\epsilon$) 347 (–1.3), 284 (–19.7), 255 (+4.4), 228 (–3.0), 202 (+46.2) nm.

Guajadial C (21). ECD (c 4.6×10^{-4} M, MeCN) λ_{max} ($\Delta\epsilon$) 345 (+1.4), 280 (+11.9), 252 (–2.3), 218 (–10.5), 207 (+27), 191 (–12.0) nm.

Guajadial D (22). ECD (c 4.4×10^{-4} M, MeCN) λ_{max} ($\Delta\epsilon$) 340 (–1.1), 297 (–1.4), 261 (+3.9), 214 (+16.9) nm.

Guajadial E (23). ECD (c 4.2×10^{-4} M, MeCN) λ_{max} ($\Delta\epsilon$) 344 (–3.3), 285 (–15.0), 259 (+5.8), 211 (+27.3), 191 (–9.0) nm.

Guajadial F (24). ECD (c 4.9×10^{-4} M, MeCN) λ_{max} ($\Delta\epsilon$) 349 (+1.2), 277 (+25.0), 247 (–3.5), 215 (+20.6), 192 (–43.0) nm.

Guajavadial A (25). Colourless oil; $[\alpha]_D^{26} -33$ (c 0.2, CHCl_3); UV (MeCN) λ_{max} ($\log \epsilon$) 280 (4.3) nm; ECD (c 1.1×10^{-4} M, MeCN) λ_{max} ($\Delta\epsilon$) 340 (–2.4), 284 (–9.8), 246 (+1.7), 191 (+31.2) nm; IR (KBr) ν_{max} 3447, 2957, 2923, 2851, 1635, 1442, 1307, 1219, 772 cm^{-1} ; ^1H and ^{13}C NMR data, see Supplementary Table S2.6; (–) MS-ESI m/z 405.3 $[\text{M} - \text{H}]^-$; (–) HR-MS-ESI m/z 405.1688 $[\text{M} - \text{H}]^-$ (calcd for $\text{C}_{25}\text{H}_{25}\text{O}_5$, 405.1707).

ECD Calculations. For details of the ECD calculation for compounds 1–4, see Supplementary S4.

PDE4D Inhibitory Screening Assays. The protocols for expression, purification, and enzymatic assays of PDE4D2 were similar to those we described previously³¹. More details about the experimental procedures are provided in Supplementary S3.

References

- Kozuka, M. *et al.* The granulation-inhibiting principles from *Eucalyptus globulus* Labill. II. The structures of euglobal Ia1, Ia2, Ib, Ic, Ia, Iib and Iic. *Chem. Pharm. Bull.* **30**, 1952–1963 (1982).
- Nishizawa, M. *et al.* Macrocarpals: HIV-reverse transcriptase inhibitors of *Eucalyptus globulus*. *Tetrahedron Lett.* **33**, 2983–2986 (1992).
- Osawa, K., Yasuda, H., Morita, H., Takeya, K. & Itokawa, H. Macrocarpals H, I, and J from the leaves of *Eucalyptus globulus*. *J. Nat. Prod.* **59**, 823–827 (1996).
- Yin, S. *et al.* Eucalyptals A–C with a new skeleton isolated from *Eucalyptus globulus*. *Org. Lett.* **9**, 5549–5552 (2007).
- Yang, S.-P. *et al.* Potent HGF/c-Met axis inhibitors from *Eucalyptus globulus*: the coupling of phloroglucinol and sesquiterpenoid is essential for the activity. *J. Med. Chem.* **55**, 8183–8187 (2012).
- Yang, X.-L., Hsieh, K.-L. & Liu, J.-K. Guajadial: an unusual meroterpenoid from guava leaves *Psidium guajava*. *Org. Lett.* **9**, 5135–5138 (2007).
- Fu, H.-Z., Luo, Y.-M., Li, C.-J., Yang, J.-Z. & Zhang, D.-M. Psidials A–C, three unusual meroterpenoids from the leaves of *Psidium guajava* L. *Org. Lett.* **12**, 656–659 (2010).
- Gao, Y. *et al.* Isolation and biomimetic synthesis of (\pm)-guajadial B, a novel meroterpenoid from *Psidium guajava*. *Org. Lett.* **14**, 5936–5939 (2012).
- Shao, M. *et al.* Psiguadials A and B, two novel meroterpenoids with unusual skeletons from the leaves of *Psidium guajava*. *Org. Lett.* **12**, 5040–5043 (2010).
- Shao, M. *et al.* Guajadial A and psiguadials C and D, three unusual meroterpenoids from *Psidium guajava*. *Org. Lett.* **14**, 5262–5265 (2012).
- Jian, Y.-Q. *et al.* Guapsidial A and guadials B and C: three new meroterpenoids with unusual skeletons from the leaves of *Psidium guajava*. *Chem. Eur. J.* **21**, 9022–9027 (2015).
- Liu, H. X. *et al.* Isolation and biomimetic total synthesis of tomentodiones A–B, terpenoid-conjugated phloroglucinols from the leaves of *Rhodomyrtus tomentosa*. *RSC Adv.* **6**, 48231–48236 (2016).
- Zhang, Y.-L. *et al.* Rhodomyrtilals A and B, two meroterpenoids with a triketone-sesquiterpene-triketone skeleton from *Rhodomyrtus tomentosa*: structural elucidation and biomimetic synthesis. *Org. Lett.* **18**, 4068–4071 (2016).
- Liu, C. *et al.* Meroterpenoids with new skeletons from *Myrtus communis* and structure revision of myrtucommulone K. *Org. Lett.* **18**, 4004–4007 (2016).
- Hu, L. Z. *et al.* (\pm)-Japonicols A–D, acylphloroglucinol-based meroterpenoid enantiomers with anti-KSHV activities from *Hypericum japonicum*. *J. Nat. Prod.* **79**, 1322–1328 (2016).
- Hu, L. Z. *et al.* Filicinic acid based meroterpenoids with anti-Epstein-Barr virus activities from *Hypericum japonicum*. *Org. Lett.* **18**, 2272–2275 (2016).
- Yang, X.-W., Li, Y.-P., Su, J., Ma, W.-G. & Xu, G. Hyperjapones A–E, terpenoid polymethylated acylphloroglucinols from *Hypericum japonicum*. *Org. Lett.* **18**, 1876–1879 (2016).
- Singh, I. P. & Bharate, S. B. Phloroglucinol compounds of natural origin. *Nat. Prod. Rep.* **23**, 558–591 (2006).
- Xu, R., Snyder, J. K. & Nakanishi, K. Robustadials A and B from *Eucalyptus robusta*. *J. Am. Chem. Soc.* **106**, 734–736 (1984).
- Lal, K., Zarate, E. A., Youngs, W. J. & Salomon, R. G. Total synthesis necessitates revision of the structure of robustadials. *J. Am. Chem. Soc.* **108**, 1311–1312 (1986).
- Salomon, R. G., Lal, K., Mazza, S. M., Zarate, E. A. & Youngs, W. J. The total synthesis of robustial A and B dimethyl ethers. *J. Am. Chem. Soc.* **110**, 5213–5214 (1988).
- Koser, S., Hoffmann, H. M. R. & Williams, D. J. Stereoselective synthesis of precursors of naturally occurring robustadials A and B. *J. Org. Chem.* **58**, 6163–6165 (1993).
- Majewski, M., Irvine, N. M. & Bantle, G. W. Stereoselective synthesis of dimethylrobustadials. *J. Org. Chem.* **59**, 6697–6702 (1994).
- Tanaka, T. *et al.* Total synthesis of (–)-macrocarpal C. Stereoselective coupling reaction with a novel hexasubstituted benzene Cr(CO)₃ complex as a biomimetic chiral benzyl cation equivalent. *J. Org. Chem.* **63**, 9782–9793 (1998).
- Tran, D. N. & Cramer, N. Biomimetic synthesis of (+)-ledene, (+)-viridiflorol, (–)-palustrol, (+)-spathulenol, and psiguajadial A, C, and D via the platform terpene (+)-bicyclogermacrene. *Chem. Eur. J.* **20**, 10654–10660 (2014).
- Lam, H. C., Spence, J. T. J. & George, J. H. Biomimetic total synthesis of hyperjapones A–E and hyperjapones A and C. *Angew. Chem. Int. Ed.* **55**, 10368–10371 (2016).
- Lawrence, A. L. *et al.* A short biomimetic synthesis of the meroterpenoids guajadial and psidial A. *Org. Lett.* **12**, 1676–1679 (2010).
- Burgin, A. B. *et al.* Design of phosphodiesterase 4D (PDE4D) allosteric modulators for enhancing cognition with improved safety. *Nat. Biotechnol.* **28**, 63–70 (2010).
- Fabbri, L. M., Beghe, B., Yasothan, U. & Kirkpatrick, P. Roflumilast. *Nat. Rev. Drug Discovery* **9**, 761–762 (2010).
- Cheng, Z.-B. *et al.* Prostaglandin derivatives: nonaromatic phosphodiesterase-4 inhibitors from the soft coral *Sarcophyton ehrenbergi*. *J. Nat. Prod.* **77**, 1928–1936 (2014).
- Lin, T.-T. *et al.* Prenylated coumarins: natural phosphodiesterase-4 inhibitors from *Toddalia asiatica*. *J. Nat. Prod.* **77**, 955–962 (2014).
- Liu, X. *et al.* Selaginpulvilins A–D, new phosphodiesterase-4 inhibitors with an unprecedented skeleton from *Selaginella pulvinata*. *Org. Lett.* **16**, 282–285 (2014).
- Fuerstner, A. & Hannen, P. Platinum- and gold-catalyzed rearrangement reactions of propargyl acetates: total syntheses of (–)- α -cubebene, (–)-cubebol, sesquicarene and related terpenes. *Chem. Eur. J.* **12**, 3006–3019 (2006).
- Gao, Y. *et al.* Guajadials C–F, four unusual meroterpenoids from *Psidium guajava*. *Nat. Prod. Bioprospect.* **3**, 14–19 (2013).
- Qin, X. J. *et al.* Cytotoxic meroterpenoids with rare skeletons from *Psidium guajava* cultivated in temperate zone. *Sci. Rep.* **6**, 32748–32756 (2016).
- Li, C. J., Ma, J., Sun, H., Zhang, D. & Zhang, D. M. Guajavadimer A, a dimeric caryophyllene-derived meroterpenoid with a new carbon skeleton from the leaves of *Psidium guajava*. *Org. Lett.* **18**, 168–171 (2016).
- Shu, J., Chou, G. & Wang, Z. Two new benzophenone glycosides from the fruit of *Psidium guajava* L. *Fitoterapia* **81**, 532–535 (2010).
- Thuaytong, W. & Anprung, P. Bioactive compounds and prebiotic activity in Thailand-grown red and white guava fruit (*Psidium guajava* L.). *Food Sci. Technol. Int.* **17**, 205–212 (2011).
- Khadhri, A., El Mokni, R., Almeida, C., Nogueira, J. M. F. & Araújo, M. E. M. Chemical composition of essential oil of *Psidium guajava* L. growing in Tunisia. *Ind. Crop. Prod.* **52**, 29–31 (2014).

Acknowledgements

The authors thank the National High Technology Research and Development Program of China (863 Project, No. 2015AA020928), the Guangdong Natural Science Funds for Distinguished Young Scholar (No. 2014A030306047), the National Natural Science Foundation of China (Nos 81573302 and 81402813), and the Science and Technology Planning Project of Guangdong Province, China (No. 2015A020211007) for providing financial support to this work.

Author Contributions

G.-H.T. and Z.D. contributed equally to this work. They conducted the main experiments, analyzed data, and wrote the manuscript; Y.-Q.G. conducted the PDE4D inhibitory screening assays; Z.-B.C. did the ECD calculations; C.-J.Z. assisted the PDE4D inhibitory screening assays; S.Y. designed the experiments and revised and polished this manuscript. All authors reviewed the manuscript.

Additional Information

Supplementary information accompanies this paper at doi:[10.1038/s41598-017-01028-4](https://doi.org/10.1038/s41598-017-01028-4)

Competing Interests: The authors declare that they have no competing interests.

Publisher's note: Springer Nature remains neutral with regard to jurisdictional claims in published maps and institutional affiliations.



Open Access This article is licensed under a Creative Commons Attribution 4.0 International License, which permits use, sharing, adaptation, distribution and reproduction in any medium or format, as long as you give appropriate credit to the original author(s) and the source, provide a link to the Creative Commons license, and indicate if changes were made. The images or other third party material in this article are included in the article's Creative Commons license, unless indicated otherwise in a credit line to the material. If material is not included in the article's Creative Commons license and your intended use is not permitted by statutory regulation or exceeds the permitted use, you will need to obtain permission directly from the copyright holder. To view a copy of this license, visit <http://creativecommons.org/licenses/by/4.0/>.

© The Author(s) 2017